4.4 Profile Loss Coefficient

The profile loss coefficient is a modified form of the Ainley-Mathieson [41] model. It can be represented as

$$Y_p = K_{\text{mod}} K_{inc} K_M K_p K_{RE} \{[Y_{p1} + \xi^2 (Y_{p2} - Y_{p1})](5t_{\max}/c)^{\xi} - \Delta Y_{TE}\} \qquad (4\text{-}21)$$

K_{mod} is an experience factor suggested by Kacker and Okapuu [43] to adjust the Ainley-Mathieson model to account for the superior performance of modern designs due to improved design technology. They suggest a value of 1.0 for older designs and 0.67 for modern, highly optimized designs. The Ainley-Mathieson model includes the trailing edge loss specifically assuming that $t_2 = 0.02s$. Since the trailing edge loss is treated separately in the present model, ΔY_{TE} subtracts the trailing edge loss coefficient computed by the present trailing edge loss model for $t_2 = 0.02s$. The term involving $t_{\max}$ corrects the loss from the Ainley-Mathieson source data, which had $t_{\max}/c = 0.2$. The other terms in Eq. (4-21) are

K_{inc} = correction for off-design incidence effects
K_M = correction for Mach number effects
K_p = correction for compressibility effects
K_{RE} = correction for Reynolds number effects
Y_{p1} = profile loss coefficients for nozzle blades ($\beta_1 = 90°$)
Y_{p2} = profile loss coefficients for impulse blades ($\alpha'_2 = \beta_1$)
$\xi = (90° - \beta_1)/(90° - \alpha'_2)$

Figure 4-3 shows the nozzle blade profile loss coefficient, Y_{p1}, as a function of the pitch-to-chord ratio, including the Ainley-Mathieson graphical correlation and an empirical model that accurately approximates that correlation in analytical form. Note that the empirical model extrapolates beyond the limits of the graphical correlation so that it is usable over a wider range of applications. The location of the minimums of the curves is approximated by

$$(s/c)_{\min} = 0.46 + \alpha'_2/77; \quad \alpha'_2 \le 30° \qquad (4\text{-}22)$$

$$(s/c)_{\min} = 0.614 + \alpha'_2/130; \quad \alpha'_2 > 30° \qquad (4\text{-}23)$$

The loss coefficient is approximated by

$$Y_{p1} = A + BX^2 + CX^3; \quad \alpha'_2 \le 30° \qquad (4\text{-}24)$$

$$Y_{p1} = A + B|X|^n; \quad \alpha'_2 > 30° \qquad (4\text{-}25)$$

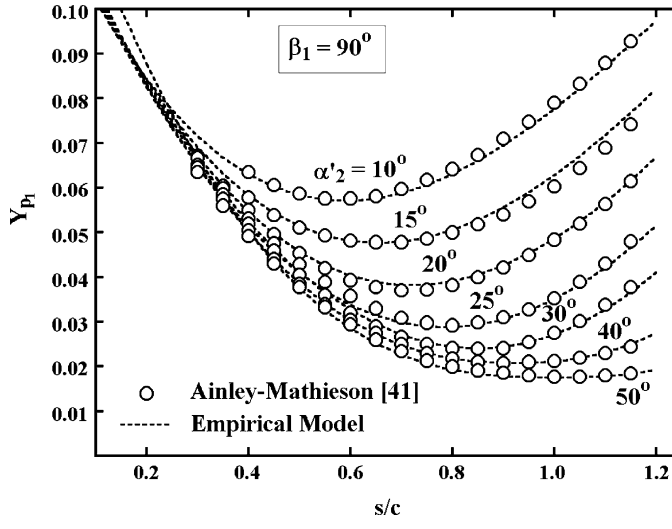

FIGURE 4-3. Nozzle Blade Profile Loss Model

The parameters used in this empirical model are defined as follows

$$X = s/c - (s/c)_{\min} \tag{4-26}$$

$$n = 1 + \alpha'_2/30 \tag{4-27}$$

$$A = 0.025 + (27 - \alpha'_2)/530; \quad \alpha'_2 \le 27^\circ \tag{4-28}$$

$$A = 0.025 + (27 - \alpha'_2)/3085; \quad \alpha'_2 > 27^\circ \tag{4-29}$$

$$B = 0.1583 - \alpha'_2/1640; \quad \alpha'_2 \le 30^\circ \tag{4-30}$$

$$C = 0.08[(\alpha'_2/30)^2 - 1 \tag{4-31}$$

Figure 4-4 shows the impulse blade profile loss coefficient, Y_{p2}, as a function of the pitch-to-chord ratio, including the Ainley-Mathieson graphical correlation and an empirical model that accurately approximates that correlation in analytical form. Again, the empirical model extrapolates beyond the limits of the graphical correlation so that it is usable over a wider range of applications. The location of the minimums of the curves is approximated by

$$(s/c)_{\min} = 0.224 + 1.575(\alpha'_2/90) - (\alpha'_2/90)^2 \tag{4-32}$$

The loss coefficient is approximated by

$$Y_{p2} = A + BX^2 - CX^3 \tag{4-33}$$

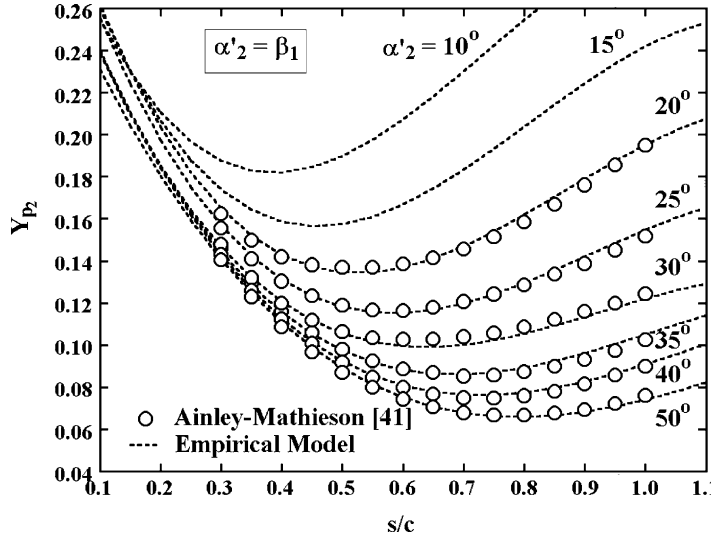

FIGURE 4-4. Impulse Blade Profile Loss Model

The parameters used in this empirical model are

$$X = s/c - (s/c)_{\min} \tag{4-34}$$

$$A = 0.242 - \alpha_2'/151 + (\alpha_2'/127)^2 \tag{4-35}$$

$$B = 0.3 + (30 - \alpha_2')/50\,; \quad \alpha_2' \le 30^\circ \tag{4-36}$$

$$B = 0.3 + (30 - \alpha_2')/275\,; \quad \alpha_2' > 30^\circ \tag{4-37}$$

$$C = 0.88 - \alpha_2'/42.4 + (\alpha_2'/72.8)^2 \tag{4-38}$$

Figure 4-5 shows the off-design incidence correction factor, K_{inc}, as a function of the ratio of the incidence angle, i, to the stalling incidence angle i_s, including the Ainley-Mathieson graphical data and an empirical model that accurately approximates that data in analytical form. Note that the empirical model extrapolates beyond the limits of the graphical correlation so that it is usable over a wider range of applications. The empirical equations are

$$i = \beta_1 - \alpha_1' \tag{4-39}$$

$$K_{inc} = -1.39214 - 1.90738(i/i_s)\,; \quad i/i_s < -3 \tag{4-40}$$

$$K_{inc} = 1 + 0.52\,|\,i/i_s\,|^{1.7}; \quad -3^\circ \le i/i_s < 0^\circ \tag{4-41}$$

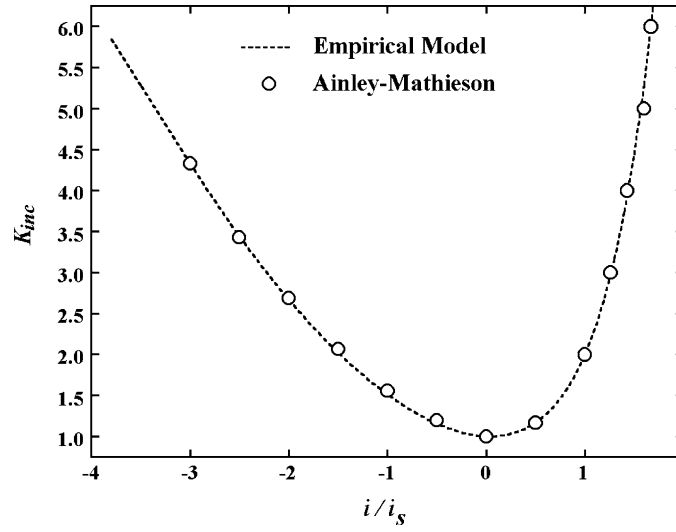

FIGURE 4-5. Off-Design Incidence Correction Factor

$$K_{inc} = 1 + (i/i_s)^{(2.3+0.5i/i_s)}; \quad 0° \le i/i_s < 1.7° \tag{4-42}$$

$$K_{inc} = 6.23 - 9.8577(i/i_s - 1.7); \quad i/i_s \ge 1.7° \tag{4-43}$$

An upper limit of $K_{inc} \le 20$ is required. The stalling incidence angle is a function of α_2', ξ and s/c, where

$$\xi = (90 - \beta_1)/(90 - \alpha_2') \tag{4-44}$$

It is computed from a reference value, $i_{sr}(\alpha_2', \xi)$, corresponding to $s/c = 0.75$ and a correction term, $\Delta i_s(\alpha_2', s/c)$, to adjust it to other values of s/c, i.e.,

$$i_s = i_{sr}(\alpha_2', \xi) + \Delta i_s(\alpha_2', s/c) \tag{4-45}$$

Figure 4-6 shows the stalling incidence for $s/c = 0.75$ as a function of the ratio of α_2' and ξ including the Ainley-Mathieson graphical data and an empirical model that accurately approximates that data in analytical form. Note that the empirical model extrapolates beyond the limits of the graphical correlation so that it is usable over a wider range of applications. The empirical equations for $\alpha_2' \le 40°$ are

$$i_{sr}(\alpha_2', \xi) = i_{s0} + A - B\xi^2 + C\xi^3 + D\xi^4; \quad \alpha_2' \le 40° \tag{4-46}$$

$$i_{s0} = 20 - (\xi + 1)/0.11 \tag{4-47}$$

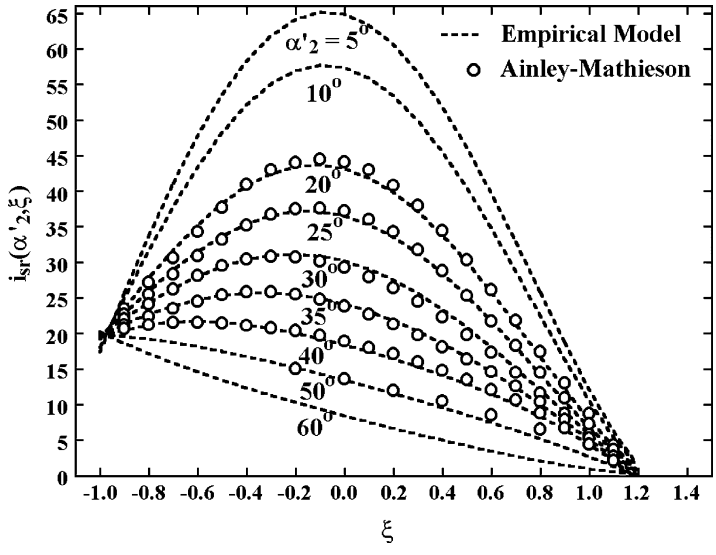

FIGURE 4-6. Stalling Incidence for *s/c* = 0.75

$$A = 61.8 - (1.6 - \alpha_2'/165)\alpha_2' \tag{4-48}$$

$$B = 71.9 - 1.69\alpha_2' \tag{4-49}$$

$$C = 7.8 - (0.28 - \alpha_2'/320)\alpha_2' \tag{4-50}$$

$$D = 14.2 - (0.16 + \alpha_2/160)\alpha_2 \tag{4-51}$$

The empirical model includes an extrapolation of the Ainley-Mathieson graphical data for $\alpha_2' > 40°$, which can be encountered on occasion. This case is approximated by

$$i_{sr}(\alpha_2', \xi) = i_{s0} + \left| i_{sr}(40, \xi) - i_{s0} \right| \left| 55 - \alpha_2' \right| / 15; \quad \alpha_2' > 40° \tag{4-52}$$

Figure 4-7 shows the correction term, $\Delta i_s(\alpha'_2, s/c)$, including the Ainley-Mathieson graphical data and an empirical model that accurately approximates that data in analytical form. The empirical equations are

$$X = s/c - 0.75 \tag{4-53}$$

$$\Delta i_s = -38X - 53.5X^2 - 29X^3; \quad s/c \le 0.8 \tag{4-54}$$

$$\Delta i_s = 2.0374 - (s/c - 0.8)[69.58 - (\alpha_2'/14.48)^{3.1}]; \quad s/c > 0.8 \tag{4-55}$$

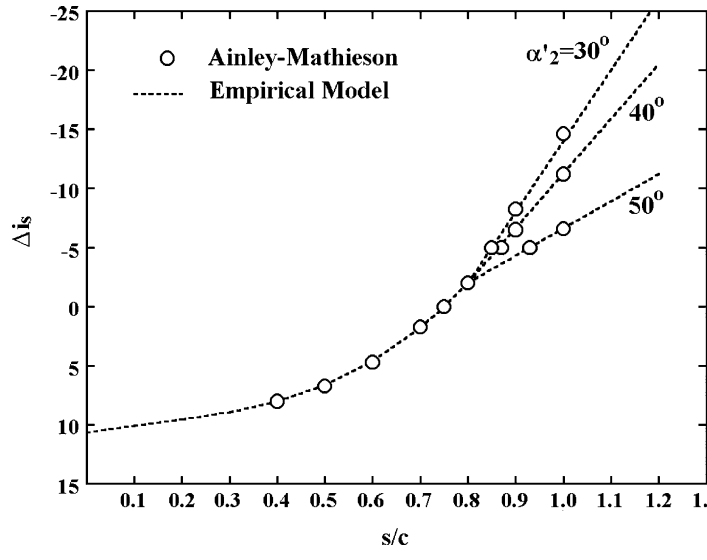

FIGURE 4-7. Stalling Incidence Correction Factor

Figure 4-8 shows the Mach number correction to the profile loss coefficient, K_M, as a function of the discharge relative Mach number, M'_2, and the ratio of the pitch to the suction surface radius of curvature, s/R_c. Both the Ainley-Mathieson graphical data and an empirical model that accurately approximates that data in analytical form are included. There is no correction

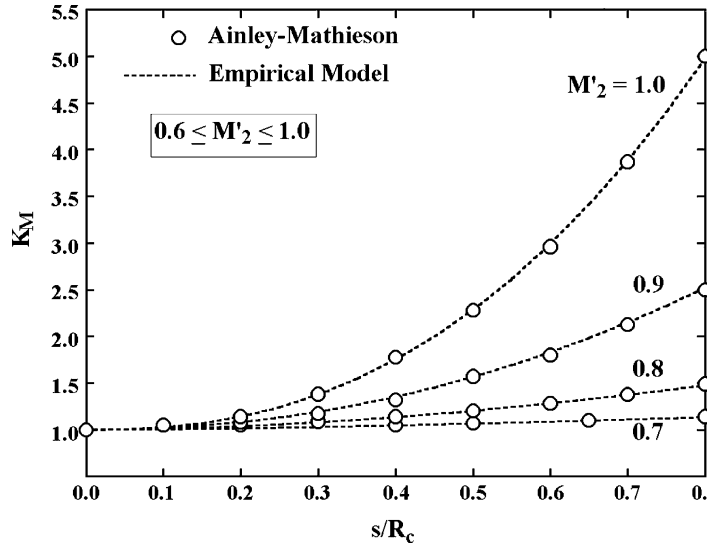

FIGURE 4-8. The Mach Number Correction

when $M'_2 \le 0.6$, i.e., $K_M = 1$. Also, the loss associated with $M'_2 > 1$ is handled separately in the supersonic expansion loss. The empirical equation used is

$$K_M = 1 + [1.65(M'_2 - 0.6) + 240(M'_2 - 0.06)^2](s/R_c)^{(3M'_2 - 0.6)} \tag{4-56}$$

The Mach number range is limited to $0.6 \le M'_2 \le 1$ when applying Eq. (4-56).

Kacker and Okapuu [43] suggest including the compressibility correction term, K_p, in Eq. (4-21) to account for the beneficial effects of Mach number levels in excess of those present in low speed cascade tests. The effect of compressibility in accelerating flow is to thin the boundary layers and suppress flow separations. Since the Ainley-Mathieson profile loss model is based on low speed cascade tests, it can be expected to be pessimistic when applied to typical turbine stage applications. Kacker and Okapuu suggest the following form.

$$K_1 = 1 - 0.625[M'_2 - 0.2 + |M'_2 - 0.2|] \tag{4-57}$$

$$K_p = 1 - (1 - K_1)(M'_1/M'_2)^2 \tag{4-58}$$

Note that $K_p = 1$ when $M'_2 \le 0.2$. For normal turbine operating conditions, this model works fairly well. But under unusual, yet feasible, conditions, this can result in profile loss coefficients essentially zero, or even negative. Kacker and Okapuu were less likely to experience such conditions in their mean-line analysis than is the case for the hub-to-shroud analysis of chapter 5. Under off-design operation, and near the end-wall contours, it is quite possible for the passage to be diffusing rather than accelerating, which can yield particularly absurd results. Hence, the Kacker and Okapuu model has been revised as follows:

$$\tilde{M}'_1 = [M'_1 + 0.566 - |0.566 - M'_1|]/2 \tag{4-59}$$

$$\tilde{M}'_2 = [M'_2 + 1 - |M'_2 - 1|]/2 \tag{4-60}$$

$$X = 2\tilde{M}'_1/[\tilde{M}'_1 + \tilde{M}'_2 + |\tilde{M}'_2 - \tilde{M}'_1|] \tag{4-61}$$

$$K_1 = 1 - 0.625[\tilde{M}'_2 - 0.2 + |\tilde{M}'_2 - 0.2|] \tag{4-62}$$

$$K_p = 1 - (1 - K_1)X^2 \tag{4-63}$$

Basically, this procedure limits $M'_2 \le 1$, $M'_1 \le 0.566$ and $X \le 1$. As a result, K_p is limited to values greater than about 0.5. For most typical turbine operating conditions, the revised model will yield results quite similar to that of Kacker and Okapuu. But it avoids the potential for absurd results in severe off-design operating conditions.

The correction term, K_{RE}, in Eq. (4-21) adjusts the profile loss coefficient for Reynolds numbers different from cascade tests upon which the model is based. Reynolds number correction schemes in axial-flow turbines are generally based on boundary layer skin friction models that relate to the total drag force on a flat plate. These models are provided in most books on boundary layer or viscous flow theory, e.g., Pai [48, 49]. The skin friction coefficients are functions of the Reynolds number, Re_L. If L is the length of the plate and μ is the viscosity,

$$Re_L = \rho CL/\mu \tag{4-64}$$

The skin friction coefficient, c_f, for laminar flow is given by

$$c_f = 1.328/\sqrt{Re_L} \tag{4-65}$$

For turbulent flow, the best available model is

$$c_f = 0.455/[\log_{10} Re_L]^{2.58} \tag{4-66}$$

Eq. (4-66) assumes that the flow is turbulent over the entire length of the plate. In practice, a portion of the flow will be laminar until the local Reynolds number exceeds the transition value, Re_{tr}. Typically, $Re_{tr} = 5 \times 10^5$ is used, but that is really an approximate value. Boundary layer transition depends on many factors, such as surface roughness, free-stream turbulence, pressure gradient, etc. When Re_L, is greater than Re_{tr}., the effective overall skin friction coefficient must be computed as a weighted average of the laminar and turbulent contributions. The skin friction coefficient attributed to the laminar portion is given by

$$c_{ftr} = 1.328/\sqrt{Re_{tr}} \tag{4-67}$$

The turbulent skin friction coefficient, c_{ft}, is given by (Eq. 4-66). For this simple flat-plate case, the ratio Re_{tr}/Re_L defines the fractional length of the laminar portion. Hence, the effective skin friction coefficient is given by

$$c_f = c_{ftr} + [c_{ft} - c_{ftr}][1 - Re_{tr}/Re_L] \tag{4-68}$$

Figure 4-9 shows the overall skin friction coefficients obtained from Eqs. (4-65), (4-66) and (4-68). The skin friction can also be influenced by surface roughness. If e is the true (peak-to-valley) roughness height, a roughness Reynolds number, Re_e, can be defined as

$$Re_e = \rho Ce/\mu \tag{4-69}$$

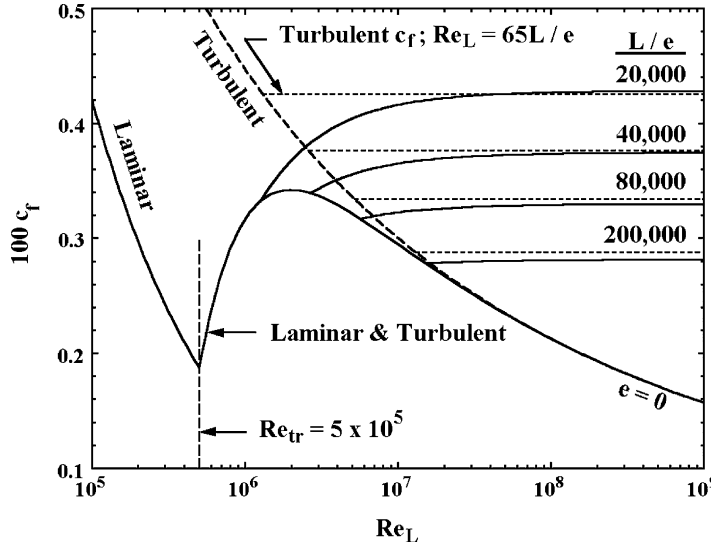

FIGURE 4-9. Boundary Layer Skin Friction Coefficient

The skin friction coefficient for a fully rough turbulent boundary layer is also well known.

$$c_{fe} = [1.89 + 1.62\log_{10}(L/e)]^{-2.5} \tag{4-70}$$

Since, roughness has no effect on c_f in the laminar portion of the boundary layer, this value must be corrected to account for the laminar portion of the boundary layer also. Hence,

$$c_f = c_{ftr} + [c_{fe} - c_{ftr}][1 - Re_{tr}/Re_L] \tag{4-71}$$

Then the effective value of the turbulent skin friction coefficient is the larger of the two values given by Eqs. (4-68) and (4-71). Skin friction coefficients for several roughness levels are shown in figure 4-9. Aungier [2] notes that the fully rough skin friction coefficient can also be evaluated from Eq. (4-66) using a value of Re_L that yields a critical value of Re_e in the range of 60 to 100. Figure 4-9 shows the result of this approach when Re_e = 65 is used.

These models are adapted to the turbine blade row application. Reynolds number corrections are normally based on the blade chord Reynolds number, Re_c, evaluated at the discharge flow conditions.

$$Re_c = \rho_2 W_2 c/\mu_2 \tag{4-72}$$

It is generally assumed that cascade empirical loss models apply to a Reynolds number of about 200,000. This lies in transition region where the skin friction models are too approximate to provide a good basis for a Reynolds number correction. Similar to Kacker and Okapuu [43], $K_{RE} = 1$ is assumed in the transition region. The present method uses a transition region defined by $1 \times 10^5 < Re_c < 5 \times 10^5$. When $Re_c < 1 \times 10^5$, K_{RE} is based on the laminar skin friction model, i.e.,

$$K_{RE} = \sqrt{(1 \times 10^5) / Re_c} \tag{4-73}$$

Similarly, when $Re_c > 5 \times 10^5$, K_{RE} is based on the turbulent skin friction model, i.e.,

$$K_{RE} = [\log_{10}(5 \times 10^5) / \log_{10}(Re_c)]^{2.58} \tag{4-74}$$

This model is extended to include surface roughness effects following Aungier [1, 2]. Pai [49] notes that roughness effects become significant when $Re_e \geq 100$, where

$$Re_e = \rho_2 W_2 e / \mu_2$$

Now define a critical blade chord Reynolds number, Re_r, above which roughness effects become significant by

$$Re_r = 100c / e \tag{4-75}$$

If Re_r is used in Eq. (4-74), the resulting value of K_{RE} is used when $Re_c > Re_r$. But surface roughness has no effect for laminar flow, so a correction similar to Eq. (4-71) is needed when $Re_r < Re_{tr}$, i.e.,

$$K_{RE} = 1 + \{[\log_{10}(5 \times 10^5) / \log_{10}(Re_r)]^{2.58} - 1][1 - (5 \times 10^5) / Re_c] \tag{4-76}$$

Figure 4-10 shows basic results from this Reynolds number correction. This model is similar to the method suggested by Kacker and Okapuu [43]. An important difference is that Kacker and Okapuu do not consider surface roughness effects. The AMDC [42] Reynolds number correction is proportional to $Re^{-0.2}$ and referenced to $Re = 2 \times 10^5$. This is based on Ainley and Mathieson [41], although that reference suggests a more severe correction for $Re < 1 \times 10^5$. The AMDC model also ignores the effects of surface roughness. One of the few published Reynolds number corrections to consider surface roughness effects is the method of Craig and Cox [44]. They note that turbine blades with standard surface finish have values of c/e in the range of 10,000

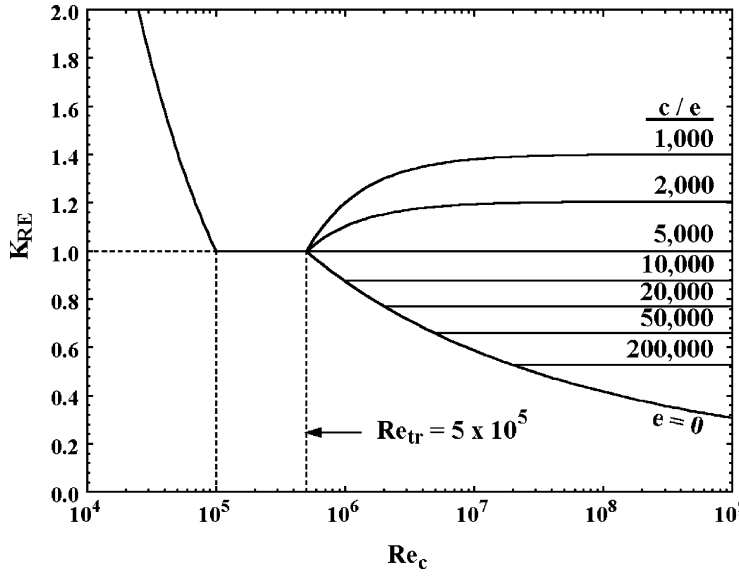

FIGURE 4-10. The Reynolds Number Correction

to 20,000, which is consistent with this writer's experience. As seen in figure 4-10, the present method will show much less Reynolds number influence for very high Reynolds numbers than methods that ignore surface roughness. It is encouraging to note that figure 4-10 shows values of K_{RE} comparable to the Craig and Cox method when surface roughness effects are significant. Indeed, any correction for Reynolds number that does not account for surface roughness should be used with extreme caution. Some rather serious high-pressure steam turbine performance deficiencies have been traced to that oversight.

4.5 Secondary Flow Loss Coefficient

The secondary flow loss coefficient is quite similar to the AMDC model reported by Dunham and Came [42] as revised by Kacker and Okapuu [43]. The lift coefficient is defined as

$$C_L = 2(\cot\alpha_1' + \cot\alpha_2')s/c \tag{4-77}$$

Eq. (4-77) may appear incorrect to some readers unless it is recalled that the flow angles conform to the blade angle convention rather than the flow field convention as discussed at the start of this chapter. The Ainley loading parameter, Z, is defined as

$$Z = (C_L c/s)^2 \sin^2\alpha_2'/\sin^3\alpha_m' \tag{4-78}$$